



## Buried plastic scintillator muon telescope

F. SANCHEZ<sup>1</sup>, G. A. MEDINA-TANCO<sup>1</sup>, J. C. D'OLIVO<sup>1</sup>, G. PAIC<sup>1</sup>, M. E. PATINO SALAZAR<sup>1</sup>, E. NAHMAD-ACHAR<sup>1</sup>, J. F. VALDES GALICIA<sup>2</sup>, A. SANDOVAL<sup>3</sup>, R. ALFARO MOLINA<sup>3</sup>, H. SALAZAR IBARGUEN<sup>4</sup>, M. A. DIOZCORVA VARGAS TREVINO<sup>5</sup>, S. VERGARA LIMON<sup>5</sup>, L. M. VILLASENOR<sup>6</sup>.

<sup>1</sup> Instituto de Ciencias Nucleares, Universidad Nacional Autónoma de México, México, D.F., C.P. 04510,

<sup>2</sup> Instituto de Geofísica, Universidad Nacional Autónoma de México, México, D.F., C.P. 04510,

<sup>3</sup> Instituto de Física, Universidad Nacional Autónoma de México, México, D.F., C.P. 04510,

<sup>4</sup> Instituto de Física, Universidad de Puebla, México, Puebla, C.P. 72570,

<sup>5</sup> Facultad de Ciencias de la Electrónica, Grupo de Robótica, Benemérita Universidad Autónoma de Puebla, Av. San Claudio y 18 Sur C. U., Edif. 182, C.P. 72570, Puebla, México,

<sup>6</sup> Universidad de Michoacán, Morelia, Mich., C.P. 58040, México.

federico.sanchez@nucleares.unam.mx

**Abstract:** Muon telescopes can have several applications, ranging from astrophysics to fundamental particle physics. We show the design parameters, characterization and end-to-end simulations of a detector composed by a set of three parallel dual-layer scintillator planes, buried at fix depths ranging from 0.30 m to 3 m. Each layer is 4 m<sup>2</sup> and is composed by 50 rectangular pixels of 4 cm × 2 m, oriented at a 90 deg angle with respect to its companion layer. The scintillators are MINOS extruded polystyrene strips with two wavelength shifting fibers mounted on machined grooves. Scintillation light is collected by multi-anode PMTs of 64 pixels, accommodating two fibers per pixel. The front-end electronics has a time resolution of 7.5 nsec. Any strip signal above threshold opens a GPS-tagged 2 micro-seconds data collection window. Separation of extensive air shower signals from secondary cosmic-ray background muons and electrons is done offline using the GPS-tagged threefold coincidence signal from surface water cerenkov detectors located nearby in a triangular array. Cosmic-ray showers above 6 PeV are selected. The data acquisition system is designed to keep both, background and signals from extensive air showers for a detailed offline analysis.

## Introduction

The Earth atmosphere is constantly hit by the cosmic radiation. After the first interaction occurs with air molecules at high altitudes, showers of secondary particles are generated and, eventually, their products may reach the ground. The exact fraction of each product at the surface level depends on the atmospheric mass overburden but, in any case, the most important components are the muonic and the electromagnetic ones. Muons are the most numerous charged particles and are mainly produced from the decay of charged mesons at heights of around 15 km. The electromagnetic component at ground consist of electrons, positrons and photons primarily from electromagnetic cascades initiated by the decay of neu-

tral and charged mesons and multiplied by pair production and Bremsstrahlung. The ratio of the electromagnetic to muon component at ground carries crucial information about the primary cosmic radiation. The number of muons at ground can be used to infer the fundamental physics involved in the first interactions points as well as the mass composition of the primary particle.

The main goal of the experimental setup presented in this work is to discriminate the muonic and electromagnetic component coming from cosmic ray showers above 6 PeV. As the background muons will be continually recorded, searches of muon excesses on the sky will also be possible.

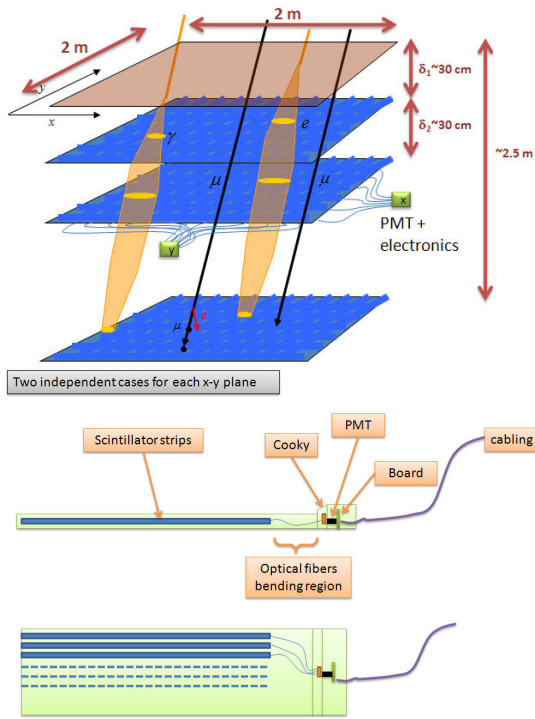


Figure 1: Schematic view of the electronic board of one detector layer. Main components are indicated.

### Experimental setup

In order to separate muons from photons, electrons and positrons the telescope has three horizontal dual-layer scintillator planes buried at different depths (see figure 1). Each layer consist of 50 scintillator strips 2 m long, 4 cm wide and 1 cm thick. In each plane, the two layers are rotated at 90 deg from each other in order to produce an effective x-y plane with 4 cm  $\times$  4 cm pixels and a covering area of 4 m<sup>2</sup>. Each scintillator strip is made of polystyrene doped with 1% PPO and 0.03% POPOP [2]. They are co-extruded with an outer layer of TiO<sub>2</sub> in order to improve reflectivity and have two wavelength shifting (WLS) fibers mounted on machined grooves.

The scintillator light coming from each layer is collected by multi-anode PMTs of 64 pixels, accommodating the two fibers of each strip on a single PMT pixel. The front-end electronics has a time resolution of 7.5 nsec. An schematic view of the

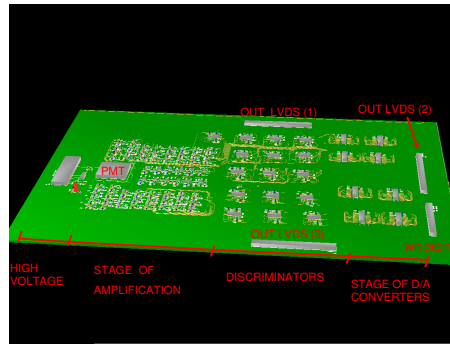


Figure 2: Schematic view of the electronic board of one detector layer. Main components are indicated.

electronic board corresponding to a single layer is shown in Figure 2 where its main components are indicated. Each channel contains an amplification stage prior to discrimination. The thresholds for each channel can be adjusted independently on real time. The detector will have six of such boards enclosed and buried in the same casing of the layer planes. Any strip signal above threshold opens a GPS-tagged 2 micro-seconds data collection window.

The three scintillator planes will be combined with a triangular array of water cerenkov detectors on the surface. The surface detectors will be 200 m apart from each other in order to produce a GPS-tagged threefold coincidence signal for cosmic ray showers of energy above 6 PeV. The separation of the background from the signal coming from showers will be performed offline.

The first two planes are planned to be buried at around 25 cm and 50 cm respectively, around the depth of maximum development for electromagnetic showers in the ground. The third plane would be buried at  $\sim$  2.5 m. However, the actual final depths are being optimized thorough Monte Carlo simulations [3], in order to maximize the discrimination potential of the telescope between muon and electromagnetically originated tracks. The muons are the most penetrating charged particles that propagate underground. Because their propagation is almost linear they are expected to cross the whole telescope volume leaving a well defined single-pixel signal in the three planes. The photons, electrons and positrons, on the other hand, de-

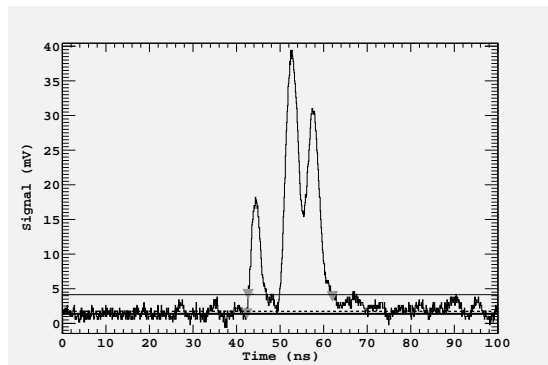


Figure 3: PMT signal from a background muon in the lab with Kuraray fibers. Lines indicate the mean, the 1 sigma and the 10 sigma noise level respectively.

velop small showers underground that may leave a two-dimensional footprint on the shallower planes of the detector.

## Measurements

The scintillation light is collected at only one end of the 2 m strips and, therefore, attenuation becomes an important factor, specially for particles hitting the opposite end of the strip. To guarantee an acceptable light output, we have tested in our laboratory fibers produced by Bicon and Kuraray. The first one is known to have a better time resolution while the second one has a higher light yield. The typical time profile of a single background muon signal, produced by the scintillator combined with Kuraray fibers, is shown in Figure 3. It can be seen that the signal is structured, being composed in this particular case by three pulses. The total width of the signal, defined as the time difference between the first and last times above  $10\sigma$  above background, is on the order of 20 nsec (see the triangles).

Individual pixels will trigger at a fixed threshold. Therefore, to compute the time resolution we compared for both fibers the rise time of the respective signals, defined as the lapse between the nearest  $1\sigma$  level crossing preceding the time of threshold (at  $10\sigma$ ). We can see from Figure 4 that the mean rise times of both fibers are close to 1 nsec.

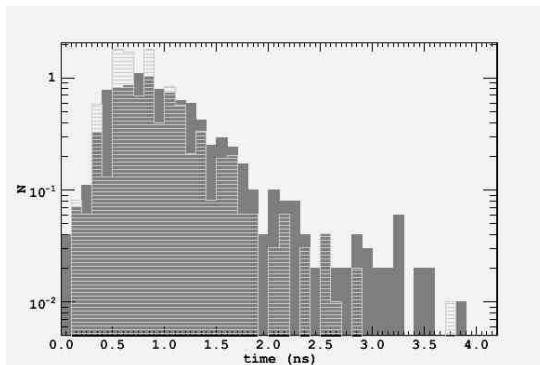


Figure 4: Rise time (see text) distribution. Solid and open histograms are with Bicon and Kuraray fibers respectively.

In order to characterize the light yield of the two types of fibers we measure in coincidence with two smaller scintillators ( $\sim 10^2 \text{ cm}^2$ ) sandwiching the strip. This setup allows to measure the output charge for background muons as a function of the distance to the PMT. In order to reproduce the short and the long attenuation lengths, typical of WLS, we calculate the attenuation length of each type of fiber by fitting a double exponential function to the medians of the charge distributions:

$$y = a_1 e^{-x/\lambda_1} + a_2 e^{-x/\lambda_2} \quad (1)$$

As an example, in Figure 5 are the spectra for three different distances and the corresponding attenuation curve fit. Results for both fibers are in Table 1. It can be seen that, besides fiber type, the gluing to the groove and the optical contact with the window of the PMT are important factors.

Fiber Type	$\lambda_1 m$	$\lambda_2 m$
B (with epotek)	0.44	8.57
K (without epotek)	0.98	5.76

Table 1: Attenuation length.

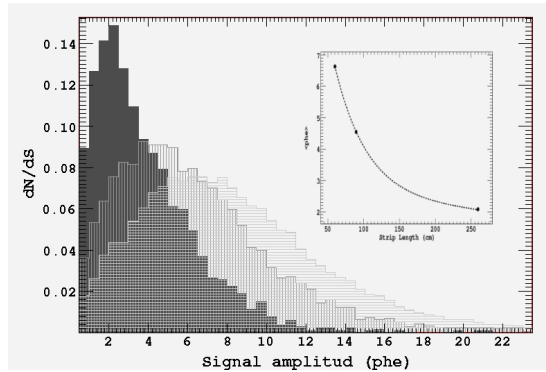


Figure 5: Charge spectra for Bicorn fiber at 60 cm, 90 cm and 260 cm.

## Simulations

As mentioned in Section 2, full Monte Carlo simulations are needed to select the depth of each detector plane in order to optimize the discrimination potential of the detector between electromagnetically originated and muon tracks. This requires the simulation of the propagation of shower particles through the atmosphere and underground up to the planes, as well as the response of the scintillator strips to the passage of charged particles. Complete details of the end-to-end simulations can be found in [3]. We show here some result of the Geant4 [1] code implemented to simulate our detector. Figure 6 is a simplified visualization of a simulated muon crossing one detector strip. As can be noted, when a charged particle enters the scintillator many photons are produced. After a few reflections off the  $\text{TiO}_2$  cover, some of them are absorbed and re-emitted by the wavelength shifter fiber and a small fraction arrives to the PMT. The various parameters characterizing the simulations are tuned to reproduce the features we measured in the laboratory. In particular, Figure 7 shows the longitudinal response of a Bicorn-like simulated strip. As can be noted, the agreement with the corresponding real case, shown in Figure 5, is good.

## Conclusions

We presented a muon telescope that is being built at present at ICN-UNAM, and that will be used to

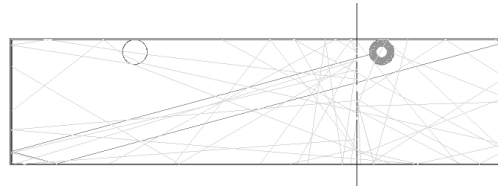


Figure 6: Simplified visualization of a simulated muon crossing a scintillator strip.

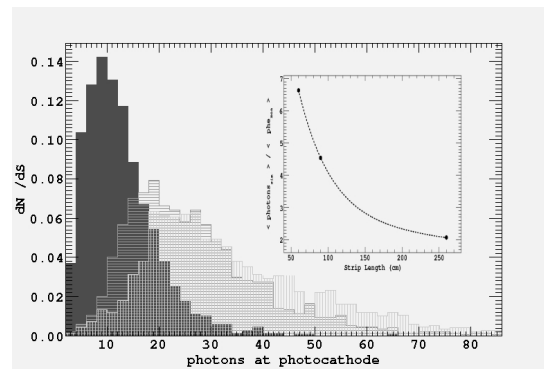


Figure 7: Simulated spectra for Bicorn fiber at 60 cm, 90 cm and 260 cm.

independently characterize the muon and electromagnetic components at ground level and to assess the magnitude of the tails of the electromagnetic distribution functions in extensive air shower. An additional goal is to measure the muonic to electromagnetic shower component ratio as a function of depth. The detector consists of a surface triangular array of water cerenkov detectors and three dual-layer scintillator planes buried at fixed depth ranging from 0.25 m to 3 m. It is planned to operate for primary cosmic rays of energy above 6 PeV.

## References

- [1] S. Agostinelli et al. . *NIM (Phys. Res. Section)*, 506:250, July 2003.
- [2] The MINOS Collaboration. *MINOS Technical Design Report*. FNAL internal document NuMI-L-337, 1998.
- [3] F. Sanchez et al. . In *30th ICRC, Merida, Mexico, 2007*, 2007.